

**NASA CONTRACTOR  
REPORT**



NASA CR-47



NASA CR-477

LOAN COPY: RETURN TO  
AFWL (WLIL-2)  
KIRTLAND AFB, N MEX

**ELECTROSTATIC MEASUREMENT  
EXPERIMENT, SCOUT VEHICLE 131-R  
(S. E. V.)**

*by P. E. Greer*

*Prepared by*  
**LING-TEMCO-VOUGHT, INC.**  
Dallas, Texas  
*for Langley Research Center*





NASA CR-477

ELECTROSTATIC MEASUREMENT EXPERIMENT,  
SCOUT VEHICLE 131-R (S.E.V.)

By P. E. Greer

Distribution of this report is provided in the interest of information exchange. Responsibility for the contents resides in the author or organization that prepared it.

Prepared under Contract No. NAS 1-3657 by  
LING-TEMCO-VOUGHT, INC.  
Dallas, Texas

for Langley Research Center

NATIONAL AERONAUTICS AND SPACE ADMINISTRATION

---

For sale by the Clearinghouse for Federal Scientific and Technical Information  
Springfield, Virginia 22151 - Price \$2.00

## ABSTRACT

Electrostatic sensors were developed, installed, and flown on Scout Vehicle 131R to experimentally evaluate vehicle electrification due to electrostatic charging. The major charge buildup was found to occur during the burning of the main booster engines. Brief background information followed by a detailed discussion on the experimental results are presented. Further electrostatic studies and experimentation are recommended.

TABLE OF CONTENTS

	<u>Page No.</u>
1.0 SUMMARY -----	1
2.0 INTRODUCTION -----	4
3.0 EXPERIMENT OBJECTIVES -----	5
4.0 SENSOR DEVELOPMENT AND APPLICATION -----	8
5.0 FLIGHT RESULTS -----	15
6.0 DISCUSSION OF RESULTS -----	19
7.0 CONCLUSIONS AND RECOMMENDATIONS -----	31

LIST OF FIGURES

<u>Figure No.</u>	<u>Figure Title</u>	<u>Page No.</u>
1	Functional Diagram - Electrostatic Potential Sensor -----	10
2	Block Diagram - Electrostatic Measurement System -----	13
3	"C" Section Potential vs. Time Curve -----	16
4	Current Voltage Characteristics of a Typical Gas-Filled Cold-Cathode Diode -----	24
5	Paschen's Law -----	24

## 1. SUMMARY

As a part of the Scout Systems Engineering Program, and NASA-LRC contracts NAS1-3657 and NAS1-3589, two types of uniquely configured electrostatic potential sensors were developed and flown on the Scout Systems Evaluation Vehicle 131-R. The purpose was to experimentally evaluate vehicle electrification during launch phases including staging. The sensors monitored electrostatic potential differences developed between electrically isolated parts of the vehicle, and measurement data was transmitted via the standard vehicle performance telemetry system. This report is a follow-on to the reference (1) development and installation report and presents an analysis of the flight data, final conclusions, and recommendations.

Because of the difference in characteristics of the electrical potentials anticipated, two types of electrostatic sensors were developed: (1) a low frequency response unit to monitor the relatively slow build-up of electrostatic voltage differences between vehicle system ground (metal structure) and electrically isolated conductive coatings on fiberglass surfaces of the "upper B" and "upper C" interstage sections, and (2) a high frequency response unit to monitor steep wave front transient voltages developed between upper and lower stages during separations.

Flight data from the "B" and "C" section (surface charge) sensors indicates maximum potential differences of 150 and 800 volts respectively were measured between system ground and the isolated conductive coatings. While potential build-up on the "C" section began about one second after first stage ignition, that on "B" section began about 43 seconds later, near first stage burnout. The "C" section maximum occurred during "trail-off"

of the first stage motor, and maximum on the "B" section occurred while reaction control jets were operating during second stage coast. Flight data from the transient sensors indicates potential differences were not detected between the upper stages and the separating lower stages during the first or second stage separations. Based on analyses of these data, it is concluded: (1) the most significant charge build-up occurs during burning of the booster engines, (2) a lesser (secondary) charge build-up is associated with operation of the reaction control motors, and (3) any potential differences developed between stages during separation are below the 500 volt threshold sensitivity of the transient sensors. And, though the maximum potential difference measured is large enough to cause arc-over, the energy level is very small--estimated at  $10^{-4}$  joules--and is several orders of magnitude below that required to directly cause misfire in pyrotechnic circuits. However, since the vehicle structure, which is systems ground, seems to be the primary charge collector, then ungrounded systems such as the ignition/destruct circuits could develop potential differences comparable to the 800 volts measured. And, while discharge of these potentials and the associated small amounts of energy directly into pyrotechnic circuits is considered insignificant, there is a remote probability that the discharge could produce ionization and initiate other arc-overs which, once initiated, could be sustained by the supply batteries. Hence, action is recommended to: (1) determine design changes for further minimizing probability of hazards due to vehicle charging, (2) investigate further any transient voltages induced at staging,

(3) investigate conductive coatings for application on vehicle surfaces to eliminate development of large potential differences, (4) obtain electrostatic data by addition of special instrumentation during other scheduled static firings of both solid fuel rocket motors and peroxide reaction control motors, and (5) conduct a repeat flight experiment with additional monitoring precautions, modified sensors and additional sensors to determine separation rates during staging.

## 2.0 INTRODUCTION

An electrostatic experiment was flown on Scout vehicle 131-R as a result of the investigations into the inflight loss of Scout vehicle 128-R. Results of those investigations indicated that certain electronic components in the vehicle destruct system may have been susceptible to premature initiation by discharge of static electricity. Based on the findings of the investigations, and in lieu of information which was to have been obtained from a LTV proposed formal study and laboratory test program, NASA included in the program plan for the Scout Systems Evaluation Vehicle (SEV), the installation of sensors to measure the possible build-up of electrostatic charges on the Scout vehicle.

The development, fabrication, and installation of the electrostatic sensors on Scout vehicle SEV-131R was conducted. The Systems Evaluation Vehicle was successfully launched from Wallops Island, Virginia on 10 August 1965. Analysis of the flight data indicates the four electrostatic sensors functioned satisfactorily.

This report describes the electrostatic experiment objectives and sensor development concepts; provides a detailed analysis and discussion of the flight data; and presents conclusions based on results of the experiment, with recommendations for follow-up action. A previous report, reference (1), provided details regarding development of the flight sensors.

### 3.0 EXPERIMENT OBJECTIVES

The objectives of the experiment were: (1) to investigate Scout vehicle electrification caused by accumulation of electrostatic charges during the launch phases, including staging, and (2) to determine the magnitudes of the resulting electrostatic potential differences developed between parts of the vehicle subsystems. These objectives were established on the basis of studies and tests conducted in support of the vehicle 128R failure analysis, and on accelerated qualitative study programs which included technical report surveys (references 3 through 10), personal contacts with past experimentors, and preliminary analysis of possible hazards due to accumulation of static electrical charges on the Scout vehicle.

With the basic objectives in mind, possible charging mechanisms were reviewed; rough estimates were made of charging rates and magnitudes of charge build-up; and flight sensor concepts and performance requirements were established. Reference (1) provides a detailed report on these items and the development of flight sensors. Excerpts from that report are again presented in this final report to assist in analysis of the flight data and evaluation of results.

Of the several sources of vehicle charging which are available during the boost phase of a standard Scout vehicle, the two considered most applicable are described as follows:

- a. The Engine Charging (or electron diffusion) theory, proposes that within the thermally ionized combustion products of rocket motors, the electrons, being more mobile than the positive ions, diffuse to the combustion chamber walls more rapidly than the positive ions (reference 3). The less mobile positive ions are then expelled

with the exhaust gases, leaving the motor housing negatively charged. Since the combustion chamber is completely enclosed in metal, the electron charge immediately flows to the outside surface, leaving a virtually field-free region within the chamber. Thus, further diffusion of electrons to the walls is not inhibited by the charge already acquired by the walls. The vehicle potential thus continues to increase until some limiting process occurs, such as corona discharge (in the atmosphere) or recirculation of positive ions from the vehicle exhaust. The majority of the positive ions, however, would be carried away by the exhaust, even when the vehicle is charged to a potential of several hundred kilovolts.

- b. Triboelectric charging or frictional charging occurs when two dis-similar materials are placed in contact and then separated (reference 3). Materials higher in the triboelectric series tend to charge positively when brought into contact with materials below them in the series and the reverse also holds true. During the launch phase for space flight, a rocket vehicle may fly through an atmosphere of charged particles consisting of meteoric and volcanic dust, cirrus cloud ice crystals, and ionospheric gaseous ions. Although any or all of the above mentioned triboelectric sources exist, reference 3 indicates that the principal triboelectric charging will result from encounters with low-altitude cirrus cloud formations. Depending on the vehicle intercepting area, the charging rate could be on the order of hundreds of milli-amps due to cirrus clouds alone.

Other charging processes include Photoelectric Charging, Plasma Effects in the Ionosphere, and Antenna Rectification. Although these processes are not to be overlooked when comparing the charging rates, they are generally considered negligible during the launch phase (references 3 and 4). Further investigations also revealed that some confusion exists in the electron diffusion theory. Recent experiments (reference 3), in which the charging of small solid-fuel rocket motors was measured during static firings, indicate that the motors often charge positively rather than negatively. In reviewing the results of a series of static firings and also actual flight experiments (reference 3), it is concluded that, although the charge build-up is large, some charging mechanism other than electron diffusion must be active to account for positive charging. A possible explanation of the positive charging is triboelectric as the solid particles in the combustion products strike the nozzle walls, or in the case of the Scout vehicle, the combustion products impinging on the jet vanes.

In regard to adverse effects of vehicle electrification on booster system performance, it was concluded that, within the atmosphere, electrostatic charging can increase vehicle potential until corona discharge occurs. And, since corona consists of a series of current pulses of fast rise time, it is a source of RF interference in the high frequency range. This corona-produced interference may disable communication systems and, in some cases, may induce spurious pulses in electronic systems controlling stage sequencing and vehicle guidance systems (references 5 and 6).

#### 4.0 SENSOR DEVELOPMENT AND APPLICATION

Due to the difference in the characteristics of the two potentials to be measured, two types of uniquely modified field mill (generating voltmeter) sensors were developed: (1) a low frequency response unit, and (2) a high frequency response transient unit. (Complete details of the development of electrostatic sensors for the Scout vehicle experiment are contained in references (1) and (2). Scout Engineering Report No. 23.233, "Development of Electrostatic Sensors for Scout Systems Evaluation Vehicle, 131R" dated 30 July 1965). The low frequency response unit was developed specifically to measure the relatively slow voltage build-up due to accumulation of charges on the vehicle surfaces. The high frequency response transient unit was developed specifically for monitoring steep wave front transients or oscillatory voltages during the first 100 milliseconds of the staging operation.

Operating characteristics of the two sensors are described as follows:

- a. Surface Measurements - The sensor is a generating voltmeter modified to overcome the disadvantages associated with flush mounting. A normally configured generating voltmeter is a flush mounted electric field meter consisting of a stationary electrode (stator) and a rotating electrode (rotor) and associated circuitry. The rotor and stator are configured such that as the sensor views an external electric field, the stator is alternately exposed to and shielded from the field by the rotor as it rotates at some fixed angular velocity; thus, an AC signal is induced in the stator. The AC signal is amplified and then rectified to produce a DC output proportional to the electric field at the stator.

To eliminate the extensive vehicle modifications necessary for flush mounting, the instrument was modified to remotely sense the surface potentials with only minor vehicle modifications. A fixed plate was built into the instrument and electrically connected to a conductive coating on the fiberglass surface (see reference 1). The fixed plate was then at the same potential as the coating. The rotor was located so the stator would view the electric field between the plate and the stator as shown in Figure 1. The rotor modulates the field viewed by the stator in the normal manner, and the output signal is a measure of the field produced by the fixed plate, and therefore the potential common to the fixed plate and the conductive coating. The sensor head is pressurized to prevent electrical breakdown between the electrodes at reduced pressure. As an oversimplified example, consider the fixed plate and the stator as a parallel plate capacitor. The field is  $E = v/d$ , where  $V$  is the potential difference between the fixed plate and the stator, and  $d$  is their relative separation. Then  $E$  is measured, and  $d$  is known; so the potential of the fixed plate and therefore of the conductive coating can be determined. In practice, direct calculation of surface voltage from sensor dimensions is not precise. The rotor distorts the field, and because of the size of the electrodes, edge effects introduce significant uncertainties. However, these factors were calibrated out of the system. Figure 1 is a functional diagram of the surface measurement subsystem. The sensor operated on 28 volts DC and required approximately one watt, which was supplied from the vehicle electrical

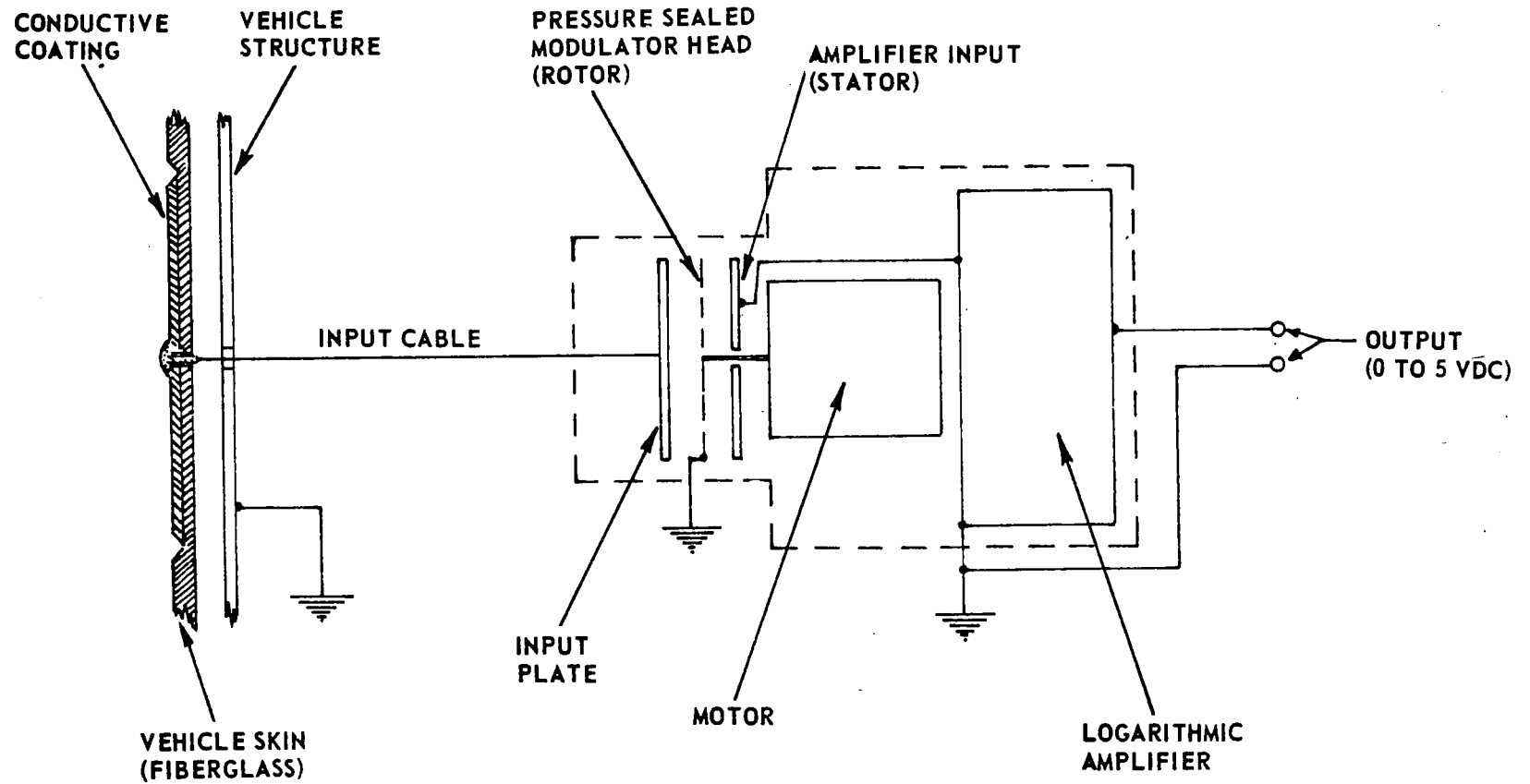


FIGURE 1 FUNCTIONAL DIAGRAM ELECTROSTATIC POTENTIAL SENSOR

system. The amplifier was a non-polarity sensitive logarithmic response unit with an input range from  $\pm 10$  volts to  $\pm 30,000$  volts, and an output of  $+0.5$  volts to  $+5.0$  volts DC.

- b. Separation Measurements - The instrument selected for the separation measurement was the basic Surface Electrical Potential Sensor, with the rotor removed, and a higher frequency linear response amplifier. The separation measurements were made during the first 80 milliseconds of stage separation. Since the potential to be measured was expected to be a short duration transient, the input required no chopping; and therefore the rotor was eliminated. In evaluating the possible transients during the first 80 milliseconds of separation, it was estimated that the pulses could vary from 2 microseconds to 80 milliseconds in rise time, and from 50 volts to 50,000 volts in amplitude. With these factors in mind, the sensor required a frequency response of at least 100 KC. Furthermore, this measurement was assigned to IRIG channel 12 (10.5 KC) subcarrier band in the "D" section telemetry System. Since Channel 12 has a frequency response of 160 cps, a pulse retention network was required to assure oscillator response to short duration transients. The pulse retention requirements were established such that 98% of the peak value of an input pulse should be retained for 5 milliseconds on the output. A linear response amplifier with a range from  $\pm 500$  volts to  $\pm 50,000$  volts was used in the sensor design. The power requirements for the transient sensors were approximately 100 milliwatts - considerably less than for the surface sensors due to the removal of the rotor and rotor driving motor.

In actual application, four sensors were required to monitor the electrostatic potentials during ascent and separation of the first two stages. Two surface measurements and two separation measurements were made as follows:

- a. Surface measurements were made on upper "B" section and upper "C" section. These were separate measurements and required two separate sensor installations and two separate telemetry channels. Because of the symmetry of the vehicle, it was concluded that any electrostatic charges which accumulate would be evenly distributed over the surfaces of the sections. Therefore, neither multiple sample points nor coating of the entire outer surface would be required for measurements to permit calculation of total charge build-up or of net effective potential.
- b. Separation measurements were made to determine maximum voltage amplitude between a "system ground point" in upper "B" and lower "B" sections at the time of stage separation. An identical measurement was made during second stage separation between upper "C" and lower "C" sections. These measurements were accomplished using the techniques and components described, plus a special cable to maintain electrical continuity between stages until a separation distance of approximately 18 inches was achieved. The time required for the stages to separate a distance of 18 inches was estimated at 80 to 100 milliseconds.

A block diagram of the entire electrostatic system is presented in Figure 2. The output of the electrostatic sensors was designed to modulate standard

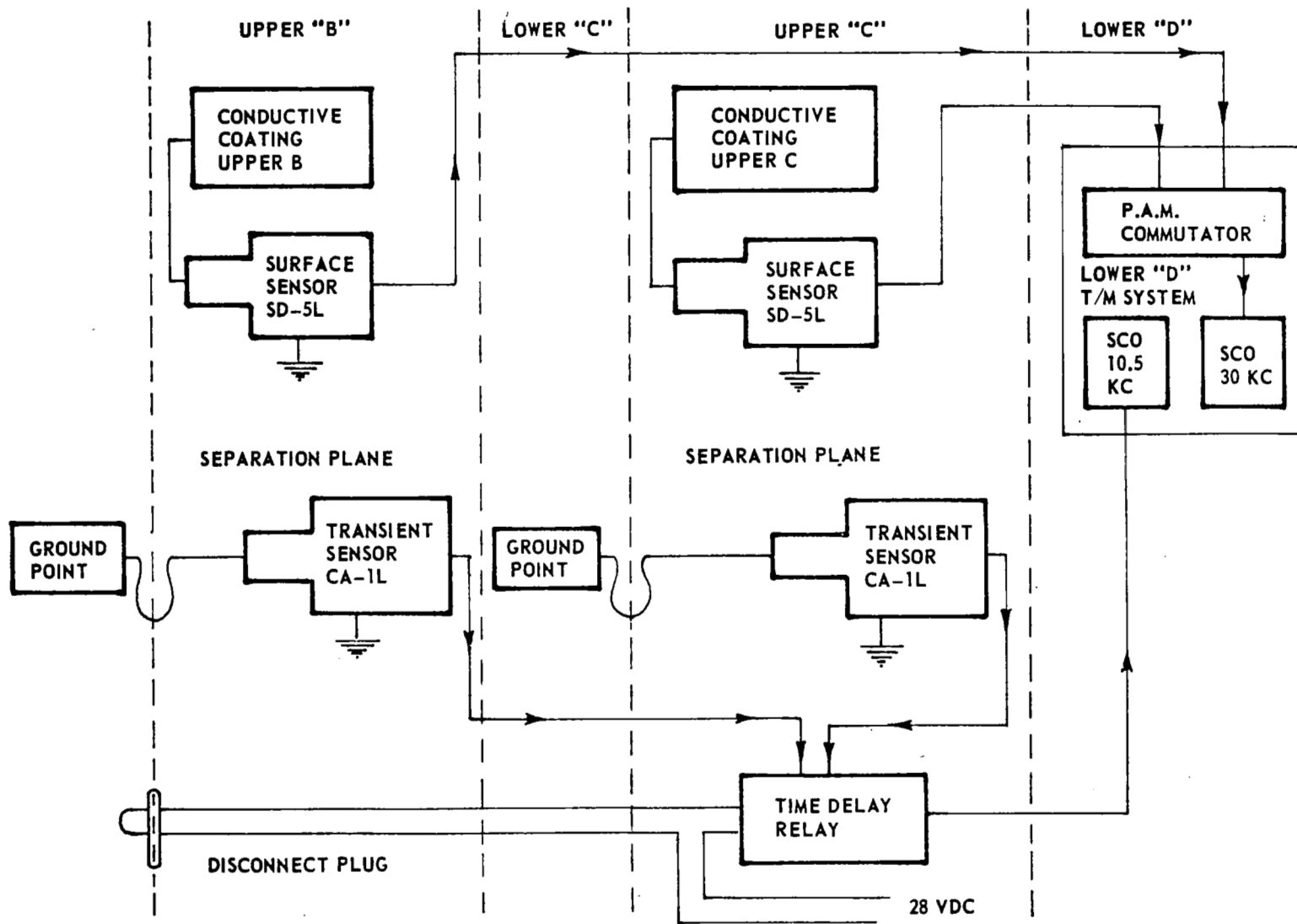


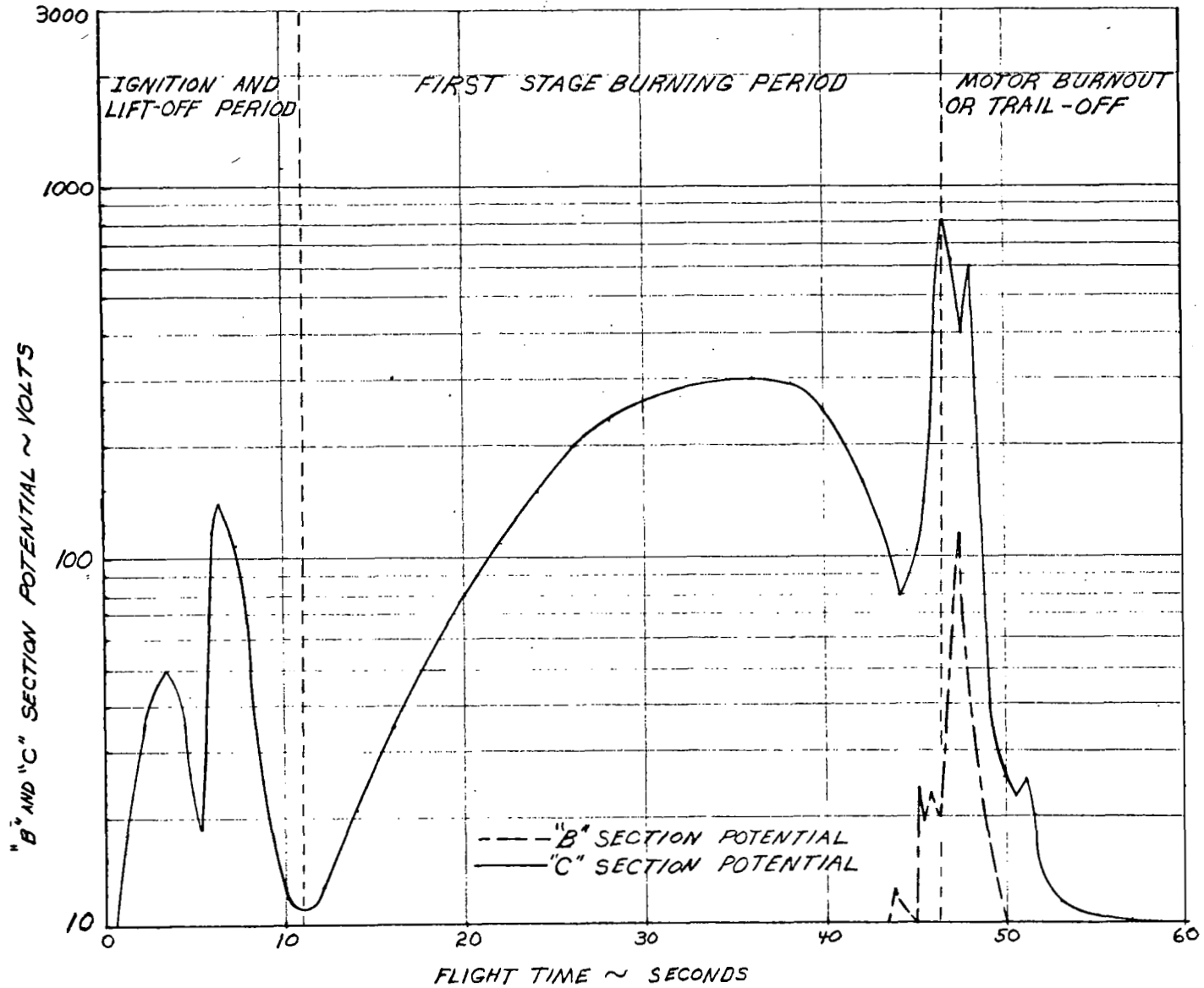
FIGURE 2 BLOCK DIAGRAM - ELECTROSTATIC MEASUREMENT SENSORS

IRIG, FM, Subcarrier Oscillators. Therefore, no intermediate signal conditioning was necessary to incorporate the electrostatic system directly into the "D" section performance telemetry system of the Scout vehicle. Two commutated channels were assigned for the surface measurements and one continuous channel was assigned for the separation measurements. The separation measurements were multiplexed on the 10.5 KC SCO of the "D" section T/M system by using a 2.5 second time delay relay. The relay was activated at second stage ignition and switched from the "B" section separation measurement to "C" section, 2.5 seconds after first stage separation.

## 5.0 FLIGHT RESULTS

To maintain clarity in the discussion of the electrostatic experiment results, the surface measurements and separation measurements are discussed separately.

- a. Electrostatic Potential Sensors (Surface Sensors) - The flight data revealed that a potential difference began to build up on the upper "C" section measurement approximately 0.6 seconds after first stage ignition. Figure 3 is a time history of the "B" and "C" section potentials measured during the first 60 seconds of flight. The "C" section surface sensor showed a continued gradual increase in surface potential during the first 36 seconds, at which time the potential had reached a value of 300 volts. The potential then started to decrease, and at 44 seconds, the "C" section potential had decayed to 80 volts. It then began a sharp increase to a value of 800 volts only 3 seconds later. The 800 volt potential began to decrease during first stage motor "trail-off" and had decayed to a zero value after 55 seconds flight time. While the "C" section sensor showed a definite electrostatic potential build-up immediately after ignition, with the variations shown in Figure 3 during first stage burning, the "B" section surface sensor showed no build-up until 43 seconds after ignition and lift-off. Then, while the "C" section potential increased from 80 to 800 volts in 3 seconds, the "B" section sensor showed a build-up from zero to 120 volts in 4 seconds. And, during first stage motor "trail-off", the "B" section potential decayed from 120 volts to zero in approximately 3 seconds; while the 800 volt



"B" AND "C" SECTION POTENTIAL DURING FIRST STAGE BURN

FIGURE NO. 3

"C" section potential reached zero about 4 seconds later.

During the first stage coast period and continuing through second stage burning, neither the "B" nor the "C" section sensors indicated any build-up of potential differences between the surface coatings and system ground (vehicle structure). However, as the second stage motor began to trail off, both the "B" and "C" section sensors indicated low amplitude, short duration potential build-ups in the 10 to 40 volt range. Also, during the second stage coast period, the "B" section sensor showed several short duration potential build-ups ranging from 10 to 150 volts in amplitude, each with a total duration (rise-time plus decay-time) of one to two seconds. After third stage ignition, the "C" section sensor indicated a somewhat erratic potential build-up which soon settled out at a 40 volt level and remained at that value during the entire third stage burning period. It decayed to zero as the motor trailed off and no further potential difference was measured during third stage coast or re-entry.

- b. Transient Electrical Potential Sensors - As previously stated, transient sensors were designed to monitor any transient electrical potentials developed between stages of the Scout vehicle from the instant of initial separation and during the first 18 inches of travel (separation) or until 2.5 seconds after second stage ignition. The flight data shows that no transients of significant magnitude were measured during separation of the first and second stages. (That is, none of magnitude greater than the 500 volt threshold or minimum sensitivity of the measurement.) Two and one-half seconds after

first stage separation, the time delay relay switched from the output of the "B" section transient sensor to the output of the "C" section transient sensor, to allow monitoring of the next staging operation. The relay switch-over produced a sharp rise time step function, with a slow decay time which did appear on the data channel and is discussed later (see Section 6.0). Flight data from the transient measurement during second stage separation also revealed no voltage transients of significant magnitude during the first 100 milliseconds, or the calculated time for 18 inches of stage separation. During that time, however, a signal dropout occurred, and it lasted for approximately 30 milliseconds. Thus the measurement data was lost during a large part of the time in which the voltage transient was anticipated. Also, at 900 milliseconds after the initial second stage separation, a 1,000 volt transient was observed, and it was followed by two other pulses of approximately 500 volts, one-half second later.

## 6.0 DISCUSSION OF RESULTS

Analysis of the flight data from the electrostatic experiment discloses several factors which appear to be anomalous or inconsistent with what might, on initial examination, be expected to occur. The first of these was the inconsistency of the data obtained from the "B" and "C" section surface sensors during first stage burning. Since the initial voltage build-up, or charging, began at 0.6 seconds after ignition of the first stage motor, it would seem the charge build-up was probably due to the first stage engine burning (Electron diffusion) and not due to triboelectric charging of external surfaces. This then would indicate that the vehicle structure was being charged while the conductive coatings on upper "B" and "C" sections remained uncharged or neutral. And the most direct result of such charging should then be that both the "B" and "C" section sensors would indicate a voltage measurement (potential difference) rather than the "C" section sensor only, as was observed. Also, consideration of triboelectric, or frictional surface charging would lead to the conclusion that the coated surface on the "B" section should be more subject to frictional charging than that on the "C" section because of the structural flare in the upper "B" section as compared to the uniform diameter of "C". Thus after about 2 or 3 seconds from lift-off, when the vehicle is at an altitude of more than 100 ft. and a velocity greater than 100 ft. per second, it might be expected that the "B" section sensor would show a greater charging rate (and potential difference) than the "C" section sensor. Also, since the "C" section sensor indicated a voltage build-up during first stage motor burning, and thus a definite charging process, it might be expected that a similar charging process and voltage build-up would occur during the second stage motor burning. However, neither "B" nor "C" section sensor

indicated a build-up as expected.

Finally, one other anomaly was observed in the data from the surface charge sensors, the anomaly being the indication of short duration potential build-ups on the "B" section during the second stage coast period. This indication of charging was considered somewhat anomalous since the data received during first stage motor burning and coast period indicated the surface potential increased during motor burning, and decayed to zero during trail-off, showing no further indication of activity (potential build-ups) during the first stage coast period. Hence, an explanation of this anomaly was required.

The above mentioned anomalies, plus the absence of a transient voltage during the first 100 milliseconds of the stage separation were carefully reviewed. Sensor installation and checkout procedures were also reviewed from the initial installation through the final checkout and removal of the plastic cover from the conductive coating two hours prior to launch. Having reviewed in detail all of the available information, the following conclusions were reached and established as providing the most logical explanations to all the observed phenomena.

First, it was concluded that the apparent inconsistency of data from the "C" and "B" section surface sensors during first stage motor firing was caused by a decrease in resistance between the "B" section conductive coating and the vehicle structure or ground. It was noted that pre-flight tests of the conductive coatings on both "B" and "C" sections, indicated a resistance to ground of  $8 \times 10^{10} \Omega$ . And also that, to prevent contamination or degradation of the insulation between the coating and vehicle ground, and to prevent oxidation of the flame-sprayed aluminum

coating, the entire surface was protected with a heavy plastic covering until two hours prior to launch. It was therefore concluded that during the two hour period while the surfaces were exposed to the salt-laden humid atmosphere, the surface of the 0.5 inch insulating gaps between the coatings and structural ground points, such as rivet heads, became contaminated with a film of salt-laden moisture (sodium chloride solution) and that immediately after first stage ignition, the upper "B" surface became further contaminated with exhaust products, such as carbon particles and metallic granules from the rising cloud of smoke, gases, and other products of combustion from first stage motor. A decrease in resistance to  $8 \times 10^8 \Omega$  would lower the RC time constant of the system to 0.2 sec. and thus prevent the detection of a potential difference between the coating and vehicle structure and its detection by the "B" section surface sensor. It was further hypothesized that, as the vehicle ascended through the atmosphere, the surface contamination or effective "low" resistance ( $\approx 10^9$  ohms) short on the input to the "B" section sensor, was removed by a combination of both heat and friction. Prior calculation indicated that the maximum dynamic pressure would occur at 40 seconds and that the surface temperature of upper "B" section would be about  $350^\circ\text{F}$  at that time.

As was previously noted, the "B" section surface sensor indicated a sharp (rapid) potential build-up began at 44 seconds after lift-off, increased to a value of 120 volts in 4 seconds, and then decayed to zero three seconds later. This activity on "B" section correlated exactly in time with the sharp potential build-up on "C" section which rose to 800 volts.

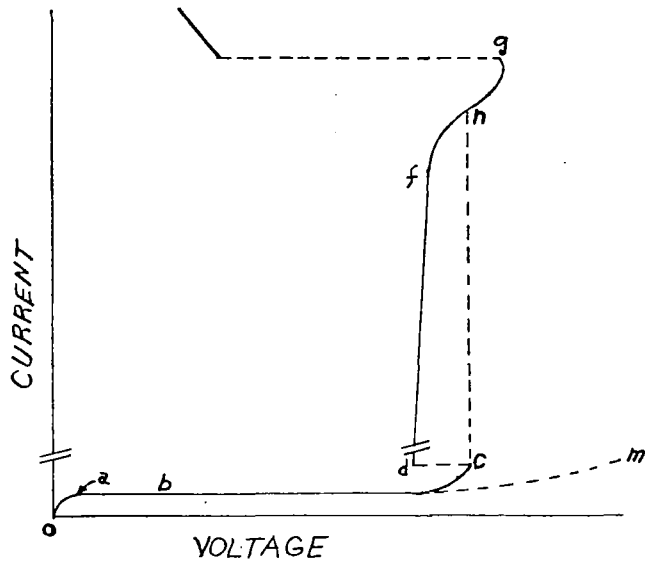
It was concluded, therefore, that the "B" section sensor was cleared of the effective input short and become operative again at approximately 44 seconds into the flight. The next question or anomaly to be considered was that of the absence of potential build-up (or lack of vehicle charging) during second stage motor burning. Considering the range of altitude through which the second stage motor burning takes place (130,000 to 260,000 ft.), it was suggested that a possible answer to this question could be that the 0.5 inch insulation gap, between the conductive coating and the vehicle structure, became insufficient, as the vehicle reached the critical pressure altitude, to prevent migration of residual ions. Thus, while the vehicle was in the critical pressure region, any charging mechanism acting was unable to develop and maintain a potential difference between the conductive coatings on the "B" and "C" sections and the vehicle structure or ground. Thus, even though the second stage engine burning was in fact charging the vehicle (as was the case during first stage burning); any potential difference developed was less than the threshold sensitivity of the sensors ( $\pm 10$  V). To elaborate further on this hypothesis, the critical pressure region was recognized as that region where all vehicle charges (or more explicitly all unbalanced charges) would be discharged or redistributed to points of greater or lesser potential because, at the reduced pressure and density, the increased mean-free-path would permit the migration of residual ions under the influence of even modest electric fields. A gas or vapor containing no ions would be a perfect insulator, and no current could flow as the result of a potential applied between two nonemitting electrodes immersed in such a gas. Ion-free gases are hypothetical, however, and because of

cosmic rays, radioactive materials in the walls of containers, photoelectric emission, and other ionizing agents in the ionosphere, some residual ions are always present. In any actual gas at low pressure, the application of potential between electrodes will produce an electric field and cause a migration of residual ions, thus producing a current flow (reference (11) and (12)).

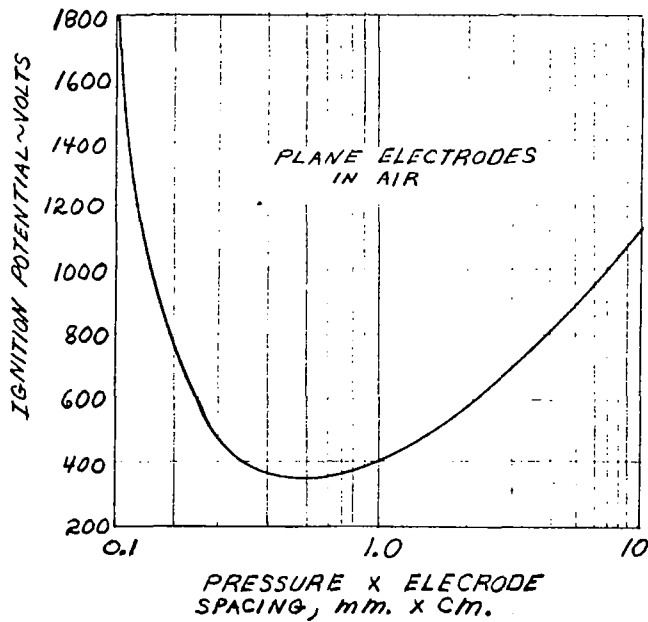
The magnitude of the current associated with the drift of residual ions evidently depends upon the rate of production of ions and upon the applied voltage. This current is sometimes called "dark current" because it is not accompanied by appreciable radiation. The relation between voltage and dark current under static conditions is shown graphically by the portion oab of the typical characteristic curve of Figure 4. That the increase of voltage over the range ab causes no increase in current, indicates that residual ions are being swept out of the gas by the electric field at the same rate as they are being created. This current is usually on the order of microamperes (reference 11).

Referring again to Figure 4, the condition obtained at point c, when the current through the discharge increases without increase in voltage, is called breakdown voltage. From what has been said, it follows that breakdown may never take place if the electrode spacing and pressures are small. This example indicates that the voltage corresponding to points c and d (Figure 4) are many times the ionizing potential.

Considering now the curve represented by Figure 5, Paschen's law states that the ignition potential is not only a function of the kind of gas and the cathode material, but also of the product of gas pressure and electrode



CURRENT-VOLTAGE CHARACTERISTICS OF A TYPICAL GAS FILLED COLD-CATHODE DIODE  
 FIGURE NO. 4



EXPERIMENTAL CURVE - BASED ON PASCHEN'S LAW.

FIGURE NO. 5

spacing (references 11 and 12). The relation between ignition potential and  $p \times d$  shown by Figure 5 is called Paschen's law, and shows that the increase of ignition voltage to the left of the minima is caused by reduction with pressure and electrode spacing of the number of molecules between the electrodes and hence of the number of collisions an electron can make in moving from the cathode to the anode. The increase to the right of the minima is caused by the facts that: (1) increase of pressure decreases the spacing between molecules and so the distance through which an electron is accelerated between collisions, and (2) increase of electrode spacing decreases the field strength at a given potential (reference 11).

Applying Paschen's law to the flight of vehicle 131R, we see that just prior to second stage burnout, the vehicle is at an altitude of approximately 260,000 feet, where the pressure is 0.594 mm - Hg. Using the 1.27 cm. insulation gap and applying the product of  $p \times d$  to Paschen's curve (Figure 5), we see that the minima has been reached on the curve and that the breakdown potential is less than 400 volts. As shown by the reference to Figure 4, the ionizing potential is many times less than the breakdown voltage, which indicates that a leakage current or dark current of several microamps could be flowing with only a very small potential between the conductive coating and the vehicle structure.

Based on this analysis, it was concluded that the lack of a voltage build-up during second stage burn could have been due to low voltage leakage currents associated with the migration of residual ions in the critical pressure region.

After S-131R had ascended through the critical pressure region and following burnout of the second stage motor, the "B" section surface sensor indicated some short duration (one to two seconds) charging periods during which peak voltages of 10 to 150 volts were reached. Further data analysis and time correlation studies revealed that the operation of the reaction control motors correlated quite well with the vehicle charging during second stage coast period. This correlation indicates that another source of vehicle charging should be added to those already considered and that future experiments may be needed on the reaction control motors to establish maximum charging rates and potentials produced by individual and/or combination motor firings.

Flight data from the transient voltage measurements included as part of the electrostatic experiment was also reviewed in detail. Since the data showed no transient voltage was detected during the separation of the first and second stage, it might be concluded that, if a voltage existed during this period, it was less than 500 volts in amplitude during the first 100 milliseconds of staging. However, the possibilities of an inoperative sensor or an inadequate installation, and therefore loss of the measurement, were also considered. In this regard, it was noted that pre-launch checkout procedures included bench tests at the launch site to insure the sensors were operating properly just prior to vehicle installation. And, because of range safety restrictions, simulation of high voltage input pulses was not permitted after the sensors were installed on the vehicle. Thus, post-installation procedures in the field were limited to checks on the remaining portions of the data channel by simulation of sensor outputs and actuation of the relay switchover previously described. As previously noted in Section 5.0, review of the

flight data disclosed a sharp rise time, step-function, voltage pulse did occur on this data channel at 2.5 seconds after first stage separation. Post-flight laboratory testing (see below) showed that this pulse resulted from relay operation at switch-over. This activity on the data channel verifies operation of the measurement system except for the sensor itself. Concerning this step-function pulse, it may be recalled the operation of the time delay relay was such that 2.5 seconds after first stage separation, the relay switched the output of the "B" section transient sensor to the output of the "C" section transient sensor. The relay operation was monitored on segment 25 of the 22 KC commutated channel in the "C" section telemetry system. The flight data shows the relay did switch over at 2.5 seconds as planned and functioned exactly as intended except for the 0.5 volt step function with a two second decay time, which occurred at the switch-over from the "B" to "C" section sensor.

To determine the exact cause of the step function, post-flight laboratory tests were conducted using a standard 28 volt relay and the back-up transient sensor. They were connected in such a way as to simulate the vehicle wiring and the laboratory tests revealed that the relay operation induced a short duration step function on the input to the sub-carrier oscillator. Repeated tests showed the amplitude of the step function varied from 0.5 volts to 1.0 volt, but the duration was never more than 5 milliseconds. By addition of external capacitance in the circuit, the 2 second decay time observed in the flight data could be produced. While the magnitude of the required external capacitance appeared to be greater than might be expected in the actual data channel wiring, it can not be said that such capacitance is not present since measurements of vehicle

wiring capacitance were not made on S-131R. Results of the tests were therefore considered to show conclusively that the step function pulse observed in the data was caused by relay switch-over.

In considering the transient measurement at second stage separation, it was again noted that no voltage pulses were detected during the first 100 milliseconds of stage separation. However, the flight records revealed that 0.9 seconds after first movement of the longitudinal accelerometer, a transient voltage of 1000 volts was recorded; and it was followed by two more pulses of approximately 500 volts, one-half second later. It was concluded, after consideration of the measurement techniques, that these pulses were possibly produced by generation of momentary electrical potentials between the third stage motor plume and the vehicle structure. The transient sensor remained quite functional during this period even though the separation lanyard was calculated to sever 100 milliseconds after third stage ignition. It was hypothesized that the trailing lanyard could have survived the direct exposure to the motor exhaust for 0.5 seconds, and that during this period, the lanyard may have been exposed to the electrical phenomena indicated on the flight records.

In summing up the results of the electrostatic experiment, it is apparent that the most outstanding results were observed during first stage motor burning. The gradual increase in overall vehicle electrification was precisely what had been anticipated, based on the vehicle charging theories established prior to development of the electrostatic sensors. It should be noted here, that even though some of the charging theories

seem to have been well founded, no firm information was available on the expected rate of surface charge accumulation, or the limiting value of charge that could occur. However, based on information obtained from studies and test reports (references 9 thru 10) on spacecraft investigations, and on measurements of effective capacity of fiberglass insulated conductive coatings, surface charging rates were estimated from as low as 100 pico-coulombs per second (100 pico-amperes) to as high as 5 milliamperes or 5 millicoulombs per second.

In studying the actual flight data, values of charging rates, of total charge accumulated, and of energy levels, were calculated from the data during first stage burn. The calculated values show that a steady charging rate of 3 milli-microamperes or 3000 pico-coulombs per second existed between 16 and 24 seconds into the flight. The maximum charging rate that was detected was 0.05 micro-amperes and occurred at 46 seconds into the flight. The maximum charge was calculated to be 0.07 micro-coulombs at an energy level of  $3 \times 10^{-5}$  ergs and occurred at 46.5 seconds after lift-off. It should be noted that the calculated values of charge and energy level were based on the measured capacitance value between the upper "C" section conductive coating and the vehicle structure. Since a discharge on a standard vehicle would be a point discharge to the surface and not involve the whole area of the conducting surface patch, it is believed that a representative discharge would involve the dissipation of energy less than  $10^{-4}$  joules. Charging values thus obtained should therefore be considered a function of this experiment only, keeping in mind that the possible Scout mission hazards created by vehicle electrification are based

on the theory that large electrical potentials can exist between the charged vehicle as a whole, and electrically isolated components or systems within the vehicle structure. Examples of isolated systems are the electrical circuits of the ignition and destruct systems and also the electrical circuits of various payload systems.

## 7.0 CONCLUSIONS AND RECOMMENDATIONS

### a. Conclusions

The electrostatic experiment data from 131R indicates the following:

- (1) Electrostatic charging does occur on the Scout vehicle during the launch phase.
- (2) This charging develops potential differences of several hundred volts between electrically isolated parts of the vehicle.
- (3) An 800-volt maximum potential difference was measured between the vehicle metal base structure and the fiberglass "C" section skin panels.
- (4) Potential differences between the upper stages and the separating lower stage were not detected. The design sensitivity of the electrostatic sensor would prevent detection of potentials less than 500 volts.
- (5) The predominant charge build-up occurs during burning of the booster engines. The measured potential difference versus time resembles the booster engine headcap pressure time history curve.
- (6) A secondary source of vehicle charging followed by rapid decay is indicated during the second stage coast. This charging appears to occur while the reaction control jets are operating.
- (7) Certain anomalies occurred in the overall data, and hypotheses as to possible causes accentuate the interplay between the environment surrounding the vehicle, altitude, the time periods

of motor burning, and voltage potential build-up. Examples are: (a) No indication of "B" section potential difference during first stage burn may be attributed to surface moisture contaminated by motor fuel products that provide sufficient conductivity to prevent potential build-up, and (b) no indication of potential build-up on "B" or "C" sections during second stage motor burning may be attributed to the bleed-off of charges at the critical pressure altitudes, where the resistance between the conductive surface plate and the structure-tie-points is sufficiently low (estimated at  $10^9$  ohms or less).

The measured 800 volt level is of a magnitude such that arc-over could occur to other lower potential areas of the vehicle. However, the energy level at a point of discharge on a standard vehicle is very small - estimated to be less than  $10^{-4}$  joules - and, even on the pyrotechnic circuits, this energy appears to be several orders of magnitude below that necessary for inadvertent misfire (as measured in tests at Cornell Labs in 1964). For an 800 volt potential difference, the energy that would be stored in the capacitance of the vehicle ground structure and the conducting surface patches used in the S-131R experimental measurements would be approximately  $10^{-3}$  joules. Since an arc-over would probably be a point discharge from the surface to the metal structure and not involve the whole area of the conducting surface patch, the  $10^{-4}$  joules was estimated for any actual discharge that might occur.

Should the vehicle metal structure be the primary charge collector, it is possible that ungrounded electrical circuits could develop a voltage or potential difference of the magnitude measured during the experiment. If arc-over did occur at altitude, the coupling of this small energy directly into the pyrotechnic circuit is not considered to be of any significance. However, the discharge could provide a mechanism for producing ionization and initiating other arc-overs which once initiated, could be sustained by the supply batteries of the pyrotechnic control circuits. For example, ions produced by electrostatic discharge between the grounded metal shell or the shield "carry-through" (ground) pin of a disconnect plug and an ungrounded circuit within that plug can provide an ionized path to permit arc-over between a 28 V supply pin and a pin in the input side of an ignition circuit.

However, the unknown charging of elements of the vehicle, the arcing of a plug shell to a critical circuit (which must be isolated from ground), the ionization created at a critical altitude, and the sustaining arc-over by other circuits must all occur in the right sequence to constitute a probable hazard. Until further data is available, the probability of occurrence of such a sequence is considered to be very remote.

b. Recommendations

Consideration of the flight results and conclusions leads to the following recommendations for follow-up action:

- (1) Perform additional experiments with special instrumentation for electrostatic data concurrent with other static firings of both solid fuel rocket motors and hydrogen peroxide reaction control motors, to establish charging rates and additional precautions for improved monitoring. It is considered probable that some of the motor firings may require use of a vacuum chamber.
- (2) Investigate the application of the conductive coatings on the vehicle surfaces to eliminate large potential differences.
- (3) Investigate further the transient voltages induced by separating two charged bodies.
- (4) It is recommended that tests and analyses be performed to determine if future design changes could be made to further minimize the probability of misfire hazards in critical circuits due to vehicle charging. It is considered probable that this may be accomplished by proper use of bleeder-resistances to avoid electrical isolation of critical circuits.
- (5) Conduct a repeat flight experiment using additional monitoring precautions and modified sensors plus the addition of sensors to determine the actual separation rate during the staging operation.

Although a considerable amount of valuable data was obtained from this experiment, more data and analyses are required. Only a continued effort to probe further into electrostatic charging

processes will yield the information necessary to eliminate the possible hazards caused by space vehicle electrification.

Information obtained from this experiment as well as that to be collected from the recommended future laboratory studies and additional flight experiments, will be useful not only to the continued reliability of the Scout program, but also to other space programs, both manned and unmanned.

## LIST OF REFERENCES

1. P. E. Greer, D. L. Edens, "Development of Electrostatic Sensors for Scout Systems Evaluation Vehicle, 131R." LTV, Scout Engineering Report No. 23.233, dated 30 July 1965.
2. N. F. Bolling, R. L. Clark, "Electrostatic Potential Sensors for Use on the NASA Scout Evaluation Vehicle, S-131R. LTV Astronautics Division Report No. 000TPO001, dated 18 August 1965.
3. E. F. Vance, L. B. Seely, J. E. Nanevicz, "Effects of Vehicle Electrification on Apollo Electro-Explosive Devices," Contract NAS9-3154, SRI Project 5101, NASA, Manned Spacecraft Center, Houston, Texas, December 1964.
4. J. B. Chown and M. G. Kennan, "Study of the Effects of Environmental Conditions on the Breakdown of Antennas at Low Pressures on a Supersonic Vehicle, "Final Report, SRI Project 2879, Contract AF19(604)-5483, Stanford Research Institute, Menlo Park, California (September 1961).
5. J. C. Axtell, "Preliminary Minuteman Electrostatic Charge Studies," Model No. WS-133A, Contract AF04(647)-580, The Boeing Company, Seattle, Washington (1963).
6. D. E. Rasque and W. J. Smith of Autonetics, "Electrostatic Phenomena on Minuteman Missile," Transactions of the Eight Symposium on Ballistic Missile and Space Technology (SECRET), Volume VI, 18 October 1963.
7. A. L. Stanley, "Electrostatic Charge Experiment," Gemini Electronics Design Note No. 411-133P-175, McDonnell Aircraft Corporation, 14 December 1964
8. K. A. Hinners, D. A. Brown, "Gemini Electrical Potential Analysis," LMSC-A014291, Lockheed Missiles and Space Company, Dept. 58-71, 22 January 1963.
9. Philip Krupen, "Measuring the Electrical Charge on a Missile in Flight," No. 69,690, Defense Documentation Center, August 1960.
10. D. A. Whittaker, "Electrostatic Characteristics of a Thor Nose Cone," No. 69,735, Defense Documentation Center, February 1962.
11. Herbert J. Reich, Ph.D., "Theory and Application of Electron Tubes," Chapter 11. McGraw-Hill, dated 1944.
12. Norman E. Gilbert, Ph.D., "Theory and Application of Electricity and Magnetism." The MacMillan Co., New York, 1950.